PLANT BIOLOGY

Eudicot plant-specific sphingolipids determine host selectivity of microbial NLP cytolysins

Tea Lenarčič,[1]* Isabell Albert,[2]* Hannah Böhm,[2]* Vesna Hodnik,[1,3]* Katja Pirc,[1] Apolonija B. Zavec,[1] Marjetka Podobnik,[1] David Pahovnik,[4] Ema Žagar,[4] Rory Pruitt,[2] Peter Greimel,[5,6] Akiko Yamaji-Hasegawa,[5,7] Toshihide Kobayashi,[5,8] Agnieszka Zienkiewicz,[9,10] Jasmin Gömann,[9,10] Jenny C. Mortimer,[11,12] Lin Fang,[11,12] Adiilah Mamode-Cassim,[13] Magali Deleu,[14] Laurence Lins,[14] Claudia Oecking,[2] Ivo Feussner,[9,10] Sébastien Mongrand,[13] Gregor Anderluh,[1]† Thorsten Nürnberger[2]†

Necrosis and ethylene-inducing peptide 1–like (NLP) proteins constitute a superfamily of proteins produced by plant pathogenic bacteria, fungi, and oomycetes. Many NLPs are cytotoxins that facilitate microbial infection of eudicot, but not of monocot plants. Here, we report glycosylinositol phosphorylceramide (GIPC) sphingolipids as NLP toxin receptors. Plant mutants with altered GIPC composition were more resistant to NLP toxins. Binding studies and x-ray crystallography showed that NLPs form complexes with terminal monomeric hexose moieties of GIPCs that result in conformational changes within the toxin. Insensitivity to NLP cytolysins of monocot plants may be explained by the length of the GIPC head group and the architecture of the NLP sugar-binding site. We unveil early steps in NLP cytolysin action that determine plant clade-specific toxin selectivity.

Necrosis and ethylene-inducing peptide 1–like (NLP) proteins are produced by bacterial, fungal, and oomycete plant pathogens, including *Pectobacterium carotovorum*, *Botrytis cinerea*, and *Phytophthora infestans*, the causal agent of the Great Irish Famine (*1*). Many NLPs are necrotizing cytolytic toxins (cytolysins) that facilitate infection of eudicot plants, but not monocot plants (*1*, *2*). The basis for host selectivity of cytolytic NLPs and their mode of action has remained obscure. We have used *Phytophthora parasitica* NLP_{Pp} and *Pythium aphanidermatum* NLP_{Pya} proteins, which have similar folds and cytolytic activities (fig. S1) (*3*), to identify and characterize the NLP toxin receptor.

NLPs are secreted into the extracellular space of host plants and target the outer leaflet of the plant plasma membrane (*1*, *4*). Cyanine3-labeled NLP_{Pp} bound *Arabidopsis* protoplasts and caused cell collapse within 10 min upon treatment (Fig. 1A). Fluorescent calcein–loaded *Arabidopsis* plasma membrane vesicles are susceptible to NLP treatment (*3*). Because vesicle pretreatment with proteases did not affect NLP cytolytic activity, we concluded that the NLP toxin receptor is not a protein (fig. S2).

NLP tertiary structures resemble those of cytolytic actinoporins (*3*, *5*, *6*). Because these toxins target metazoan-specific sphingomyelin (*7*), we assumed that NLPs target plant-specific sphingolipids. We separated tobacco leaf sphingolipids by means of high-performance thin-layer chromatography and, upon incubation with NLP_{Pya}, detected a single NLP_{Pya}-binding spot (Fig. 1B). Mass spectrometric analysis of this material revealed a glycosylinositol phosphorylceramide (GIPC) featuring trihydroxylated, monounsaturated long-chain bases and 2-hydroxylated very-long-chain fatty acids (20 to 26 C-atoms) (Fig. 1C). GIPCs are sphingolipids found in plants, fungi, and protozoa (*8*, *9*). Plant GIPCs consist of inositol phosphorylceramide (IPC) linked to glucuronic acid (GlcA-IPC) and terminal sugar residues (Fig. 1D), which vary between plants and plant tissues (*8*–*10*). Here, we identified glucosamine (GlcN) (Fig. 1C) and *N*-acetylglucosamine (fig. S3) as sugar head groups of NLP_{Pya}-binding GIPCs.

NLP_{Pya} bound purified tobacco GIPCs but not unrelated sphingolipids or phospholipids (Fig. 1B). To substantiate the NLP-GIPC interaction, we performed a sedimentation assay using multilamellar vesicles composed of 1-palmitoyl-2-oleoyl-*sn*-glycero-3-phosphocholine (POPC) and tobacco leaf GIPCs. NLP_{Pya} bound to GIPC-containing vesicles but not to those containing POPC only (Fig. 2A). To quantify NLP-GIPC interactions, we conducted surface plasmon resonance assays with GIPCs from eudicot plants *Arabidopsis*, cauliflower, or tobacco. NLP_{Pp} or NLP_{Pya} bound to all GIPC

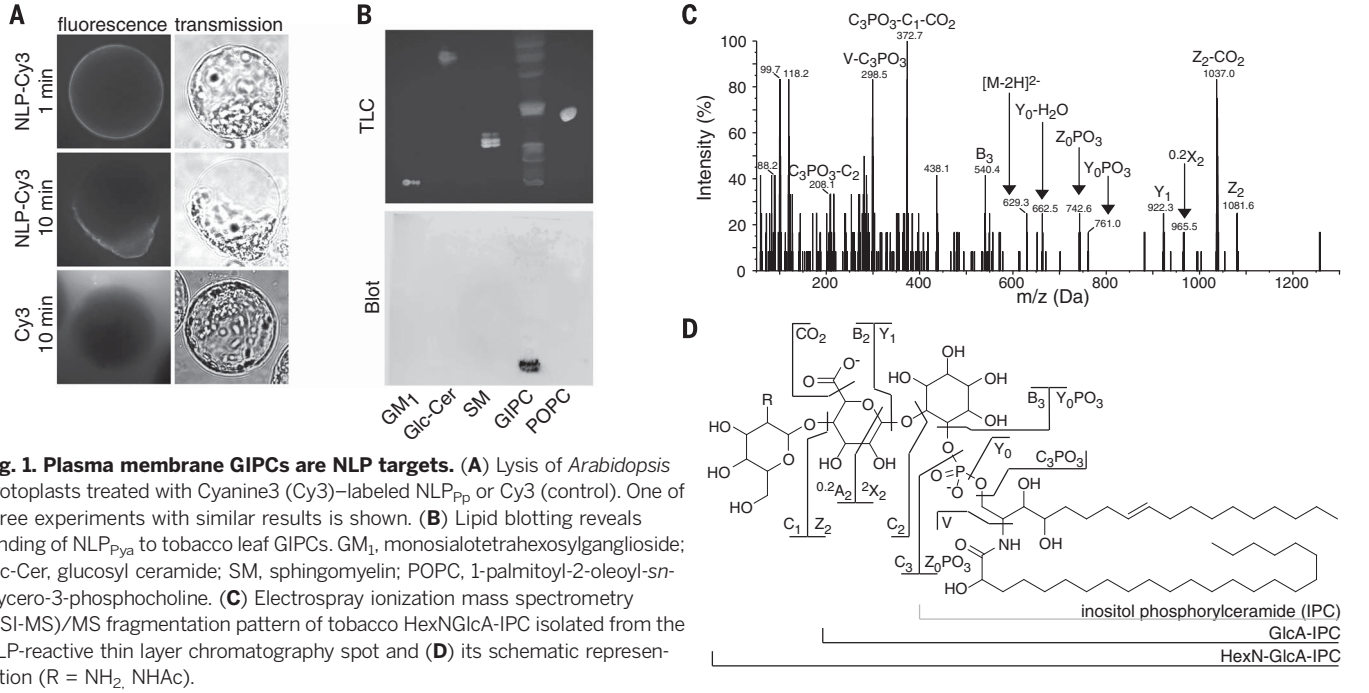

Fig. 1. Plasma membrane GIPCs are NLP targets. (**A**) Lysis of *Arabidopsis* protoplasts treated with Cyanine3 (Cy3)–labeled NLP_{Pp} or Cy3 (control). One of three experiments with similar results is shown. (**B**) Lipid blotting reveals binding of NLP_{Pya} to tobacco leaf GIPCs. GM_1, monosialotetrahexosylganglioside; Glc-Cer, glucosyl ceramide; SM, sphingomyelin; POPC, 1-palmitoyl-2-oleoyl-*sn*-glycero-3-phosphocholine. (**C**) Electrospray ionization mass spectrometry (ESI-MS)/MS fragmentation pattern of tobacco HexNGlcA-IPC isolated from the NLP-reactive thin layer chromatography spot and (**D**) its schematic representation (R = NH_2, NHAc).

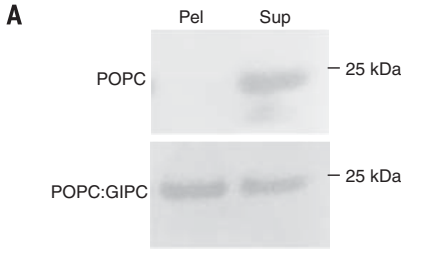

B

	K_D NLP_{Pya}	K_D NLP_{Pp}
A. thaliana	276 ± 101 nM	323 ± 103 nM
N. tabacum	448 ± 62 nM	250 ± 74 nM
B. oleracea	299 ± 162 nM	253 ± 34 nM

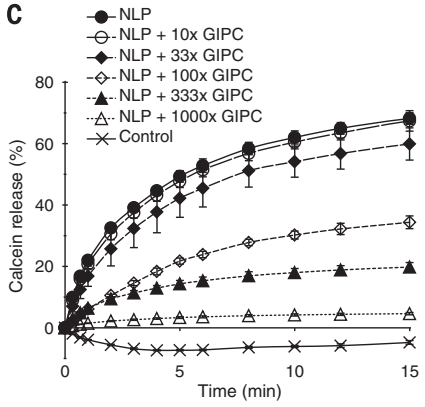

Fig. 2. Binding of NLP proteins to plant GIPCs. (**A**) NLP_{Pya} binding to POPC and POPC-GIPCs 1:1 (m:m) multilamellar vesicles monitored by means of liposome sedimentation. Pel, pellet; Sup, supernatant. (**B**) Surface plasmon resonance analysis of NLP_{Pp} or NLP_{Pya} binding to GIPCs (n = 3). (**C**) Cauliflower GIPC-mediated inhibition of NLP_{Pp}-induced (100 nM) calcein release from purified *Arabidopsis* plasma membrane vesicles. GIPCs:NLP_{Pp} molar ratios are given. Values represent means ± SD of three replicates.

preparations with dissociation constants (Fig. 2B and fig. S4) similar to NLP concentrations required to cause leaf necrosis (fig. S1D) (*3*). Soluble *Arabidopsis* GIPCs also bound chip-immobilized NLP_{Pya}, but metazoan sphingomyelin and POPC did not (fig. S5). Preincubation of NLP_{Pp} with GIPCs reduced its cytolytic activity in a GIPC-concentration–dependent manner (Fig. 2C). This suggests that saturating the toxin with its receptor prevented vesicle lysis, implying physical interaction between NLP and its receptor, GIPC.

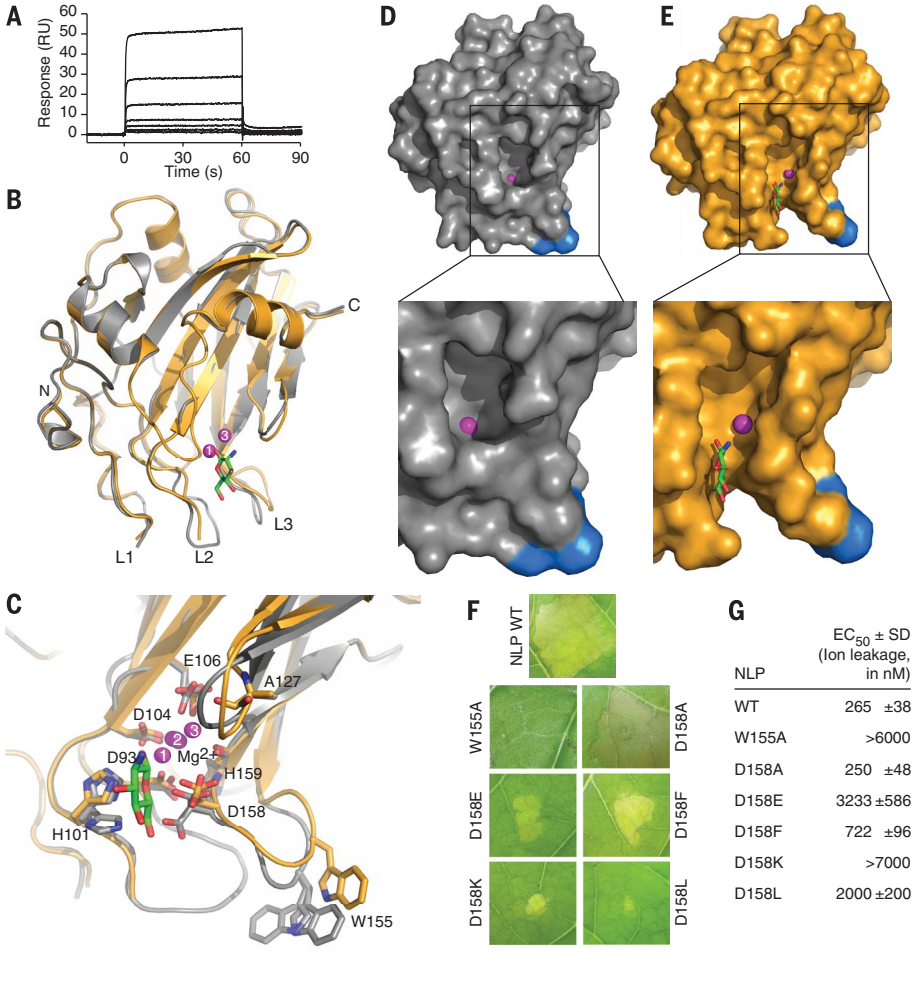

Fig. 3. Structural and functional analysis of a GlcN-NLP_{Pya} complex. (**A**) Surface plasmon resonance analysis of GlcN binding (5 mM to 78.1 μM, from top to bottom in twofold dilutions) to immobilized NLP_{Pya}. (**B** and **C**) Structural comparison of apo-NLP_{Pya} (gray) and GlcN-NLP_{Pya} complex (orange). (B) GlcN is displayed in green sticks. Loops at the bottom are designated as L1, L2, and L3. Mg^{2+} ions are shown in magenta spheres: state 1, position in apo-NLP_{Pya}; state 2, positions in other three polypeptide chains from the asymmetric unit that did not bind hexose; state 3, position in Glc-N-bound NLP_{Pya}. (C) Amino acids involved in Mg^{2+} coordination and GlcN binding and residue W155 are shown in sticks. (**D** and **E**) Conformational changes presented by protein surfaces. (D) apo-NLP_{Pya} structure (gray). (E) GlcN-bound form of NLP_{Pya} (orange). Mg^{2+} and GlcN are as in (C), and W155 is depicted as a blue surface. (**F**) Tobacco leaf necroses caused by wild-type NLP_{Pya} and NLP_{Pya} mutant proteins (200 nM). (**G**) Quantification of cell death as in (F) by means of ion leakage measurement.

We next assayed whether NLP_{Pya} can bind free sugars corresponding to the terminal saccharides found in tobacco GIPC head groups. NLP_{Pya} bound GlcN and its epimer mannosamine (ManN) (Fig. 3A and fig. S6A), but at concentrations higher than those required to bind intact GIPCs (Fig. 2B).

To address how GIPC hexoses contact NLP toxins, we determined crystal structures of NLP_{Pya} in complex with either GlcN or ManN (Fig. 3B, figs. S6B and S7, and table S1). In both cases, we found electron density indicating a bound sugar in one out of four polypeptide chains in the

[1]Department for Molecular Biology and Nanobiotechnology, National Institute of Chemistry, Hajdrihova 19, 1000 Ljubljana, Slovenia. [2]Centre of Plant Molecular Biology, Eberhard-Karls-University Tübingen, Auf der Morgenstelle 32, 72076 Tübingen, Germany. [3]Department of Biology, Biotechnical Faculty, University of Ljubljana, Jamnikarjeva 101, 1000 Ljubljana, Slovenia. [4]Department of Polymer Chemistry and Technology, National Institute of Chemistry, Hajdrihova 19, 1000 Ljubljana, Slovenia. [5]Lipid Biology Laboratory, RIKEN, Wako Saitama 351-0198, Japan. [6]Laboratory for Cell Function Dynamics, Brain Science Institute, RIKEN Institute, Wako, Saitama 351-0198, Japan. [7]Molecular Membrane Neuroscience, Brain Science Institute, RIKEN Institute, Wako, Saitama 351-0198, Japan. [8]UMR 7213 CNRS, University of Strasbourg, 67401 Illkirch, France. [9]Department of Plant Biochemistry, Albrecht-von-Haller-Institute for Plant Sciences, University of Göttingen, Germany. [10]Göttingen Center for Molecular Biosciences, University of Göttingen, Germany. [11]Joint Bioenergy Institute, Emeryville, CA 94608, USA. [12]Biosciences Division, Lawrence Berkeley National Laboratory, Berkeley, CA 94720, USA. [13]Laboratoire de Biogenèse Membranaire, UMR 5200 CNRS-Université de Bordeaux, 71 Avenue Edouard Bourlaux, 33883 Villenave-d'Ornon Cedex, France. [14]Laboratory of Molecular Biophysics at Interfaces, University of Liège, Gembloux, Belgium.
*These authors contributed equally to this work.
†Corresponding author. Email: gregor.anderluh@ki.si (G.A.); nuernberger@uni-tuebingen.de (T.N.)

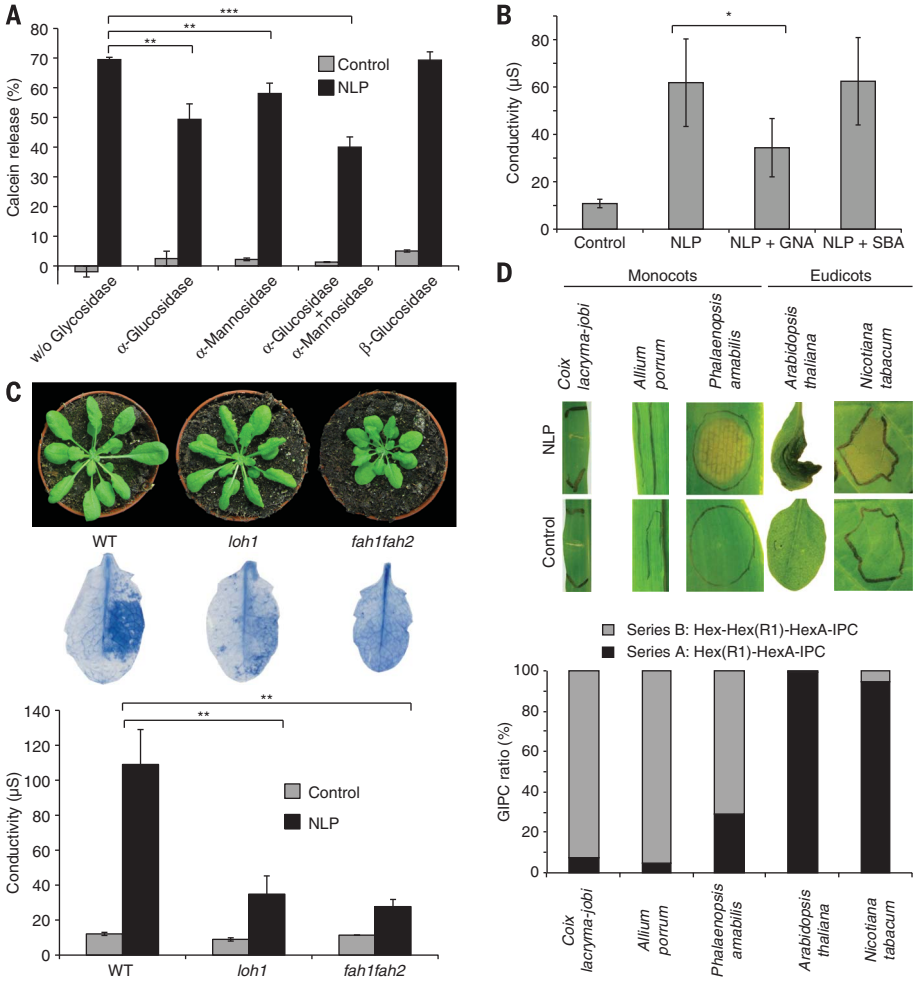

Fig. 4. Series A GIPCs determine NLP cytotoxicity. (**A**) Calcein-filled *Arabidopsis* plasma membrane vesicles pretreated (1 hour) with α-glucosidase, α-mannosidase, or β-glucosidase before addition of NLP_{Pya} or water (control). Values represent means ± SD of three replicates. Student's *t* test analyses (**$P < 0.01$, ***$P < 0.001$). (**B**) Cell death (quantified by means of ion leakage) in *Arabidopsis* Col-0 leaves treated for 6 hours with water (control) or NLP_{Pya} with and without mannose-specific GNA or galactose-specific SBA. Values are means ± SD of three replicates. Student's *t* test analyses (*$P < 0.05$). (**C**) (Top) *Arabidopsis loh1* and *fah1fah2* plants. (Middle) Cell death (Trypan blue) staining of leaves after infiltration of NLP_{Pp} or water (control). (Bottom) Cell death (quantified by means of ion leakage) in *Arabidopsis* Col-0 leaves treated with NLP_{Pya} or water (control). Values are means ± SD of three replicates. (**D**) NLP_{Pya} (1 μM)–mediated plant leaf necrosis (top). Images were taken 48 hours after infiltration. GIPC quantification (bottom) is as in (*17*) and the supplementary materials. One of three experiments with similar results is shown.

asymmetric unit. Higher B-factors for the sugar atoms relative to the protein atoms suggest partial occupancy of the sugar, which is consistent with low-affinity binding to monomeric sugars (Fig. 3A, figs. S6A and S7, and table S1). The overall fit between structures was high [root mean square deviation values for apoprotein (apo)–NLP_{Pya} and GlcN-NLP_{Pya} or ManN-NLP_{Pya}-complexes are 0.56 and 0.55 Å, respectively], but we observed structural changes attributable to sugar binding (Fig. 3, B and C, and fig. S6, B and C). Hexose moieties bound to an elongated crevice between loops L2 and L3, adjacent to a bound Mg^{2+}-ion crucial for NLP_{Pya} cytotoxicity (Fig. 3C and fig. S6C) (*3*). Sugar binding induces a conformational change in loop L3, causing widening of the L2-L3 crevice and movement of Mg^{2+} toward the center of the protein relative to its position in apo-NLP_{Pya} [Protein Data Bank (PDB) 3GNZ] (Fig. 3, B to E, and fig. S6, B and C) (*3*). L3 loops of sugar-free NLP_{Pya} chains within the same asymmetric unit exhibited conformations similar to that of apo-NLP_{Pya} (fig. S6D). Conformational rearrangements within hexose-bound NLP_{Pya} suggest that a portion of the GIPC head group is accommodated within the protein (Fig. 3, D and E, and fig. S6C). Residue W155 is placed at the bottom of loop L3 close to the hexose-binding site (Fig. 3, C to E). NLP_{Pya} W155A mutant protein exhibited neither binding to GIPCs (fig. S8) nor cytotoxic activity (Fig. 3, F and G and fig. S9), suggesting the involvement of this hydrophobic residue in interaction with the membrane. (Single-letter abbreviations for the amino acid residues are as follows: A, Ala; C, Cys; D, Asp; E, Glu; F, Phe; G, Gly; H, His; I, Ile; K, Lys; L, Leu; M, Met; N, Asn; P, Pro; Q, Gln; R, Arg; S, Ser; T, Thr; V, Val; W, Trp; and Y, Tyr. In the mutants, other amino acids were substituted at certain locations; for example, W155A indicates that tryptophan at position 155 was replaced by alanine.)

Translational movement of Mg^{2+} affects its coordination. In apo-NLP_{Pya}, Mg^{2+} is octahedrally coordinated by D93 and D104, and via four water molecules, with side chains of residues H101, E106, D158, and the main-chain carbonyl of H159 (fig. S10A and table S2) (*3*). Upon binding of either GlcN or ManN, Mg^{2+} is shifted 2.9 Å closer to E106 and becomes directly coordinated by E106 and the H159 main-chain carbonyl, whereas D93, D104, D158 side chains, and the A127 carbonyl group coordinate Mg^{2+} indirectly via four water molecules (fig. S10, B and C). The hexose is positioned between H101 and D158 side chains (Fig. 3C and fig. S6C), preventing interaction with Mg^{2+}. Mutations in D93, H101, D104, and E106 impair NLP cytotoxicity and microbial infection (*3*), which can now be explained by our structural insights.

Replacement of charged D158 with A158 did not compromise NLP cytotoxic activity, but mutation to hydrophobic F158 and L158 or charged E158 and K158 residues reduced NLP cytotoxicity (Fig. 3, F and G, and fig. S9). Space constraints in the hexose-binding cavity of these NLP_{Pya} mutants probably hinder interaction with GIPC hexose head groups. Again, hexose-NLP_{Pya} structures suggest an interpretation for the loss of function because D93, D104, and E106 are involved in Mg^{2+}-binding, whereas H101 and D158 are engaged in hexose binding (Fig. 3C; figs. S6C and S10, B and C; and table S2).

Unlike tobacco, *Arabidopsis* GIPC terminal sugars are mannose or glucose (*8*, *10*). To corroborate the role of GIPC hexose head groups in NLP function, we pretreated calcein-loaded *Arabidopsis* plasma membrane vesicles with α-glucosidase or α-mannosidase before addition of NLP_{Pya}. NLP_{Pya} caused calcein release from mock-treated vesicles, whereas calcein release from enzyme-treated vesicles was reduced (Fig. 4A). Vesicle pretreatment with β-glucosidase did not impair NLP toxicity (Fig. 4A). Thus, plant surface-exposed sugar residues are important for NLP toxicity. *Galanthus nivalis* agglutinin (GNA), a mannose-specific lectin (*11*), partially blocked NLP-mediated membrane damage, whereas galactose-specific soybean agglutinin (SBA) did not (Fig. 4B). This suggests that a mannose-specific lectin and NLP_{Pya} compete for binding to the NLP receptor.

Plants with completely disabled GIPC biosynthesis pathways are either nonviable or display developmental defects (*9*, *10*). Consequently, we used *Arabidopsis* mutants with reduced GIPC levels (fig. S11) to assess NLP sensitivity. NLP_{Pya} infiltration into leaves of ceramide synthase mutant *loh1* (LONGEVITY ASSURANCE 1 HOMOLOG1) (*12*) caused less cell death than in wild type (Fig. 4C), suggesting that lower GIPC levels promote increased toxin tolerance. GIPCs from *Arabidopsis*

gonst1 mutants lacking mannosylation (*13*) were less efficient in vesicle protection assays (fig. S12), implying reduced NLP binding. *Arabidopsis* FATTY ACID HYDROXYLASE (FAH) mutant *fah1fah2* (*14*) has reduced GIPC content (fig. S11) and altered plasma membrane organization (fig. S13), as observed in rice (*15*). When treated with NLP_{Pp}, *fah1fah2* mutants exhibited enhanced NLP toxin tolerance (Fig. 4C), suggesting that intact GIPCs or ordered plasma membranes are required for NLP cytotoxicity.

Of the two major clades of angiosperms, monocots and eudicots, only eudicots are sensitive to NLPs (*1*, *2*, *16*). Monocot GIPCs often carry three hexose units linked to IPC (series B GIPC), whereas eudicot GIPCs carry only two (series A GIPC) (*17*). Monocot *Phalaenopsis* species represent an exception in producing both series A GIPCs and series B GIPCs (Fig. 4D) (*17*). Unlike other monocots tested, *P. amabilis* developed necrotic lesions upon NLP_{Pya} treatment (Fig. 4D). Thus, it is series A GIPCs that determine plant clade-specific NLP toxin sensitivity.

NLP_{Pya} and NLP_{Pp} bind to monocot and eudicot-derived GIPCs with similar affinities (Fig. 2B and fig. S14). This is conceivable because both GIPC types carry terminal hexose residues (*17*). In model lipid membranes, both GIPCs occupy similar surface areas, despite their different hexose chain lengths (fig. S15A). This is in agreement with computer simulations, suggesting a similar perpendicular arrangement of series A (*8*) and B GIPCs. Thus, the terminal hexose residue in series B GIPCs is located further away from the membrane surface than that in series A (fig. S15B).

Microbial toxins affecting vertebrate or insect hosts often bind to glycosylated lipid receptors (*18*, *19*). We show that this mode of toxin action extends to plant hosts and that conformational changes upon binding of NLPs to GIPC sugars facilitate cytotoxicity in a manner that differs from those of other cytolysins (*5*). Although GIPC sphingolipids are abundant in plants (*8*, *10*), only eudicot and not monocot plants are sensitive to NLP cytolysins (*1*, *2*, *16*). We found the explanation to lie in the presence of series A GIPCs. Monocots that lack series A GIPCs are indeed insensitive to NLP cytolysins, but exceptions that produce both series A and B GIPCs were sensitive. Series A- and B-type GIPCs carry terminal hexose residues, but in different numbers (*8*, *17*). Binding of NLPs to series B GIPC trisaccharide terminal sugars would result in more distant positioning of the L3 loop relative to the plant membrane, impeding NLP insertion into the plasma membrane. Thus, the difference in plant sensitivity to NLP cytolysins is explained by the length of GIPC head groups and the architecture of the NLP sugar-binding site, which also excludes the branched sugar head groups found in higher-series GIPCs (*8*, *20*).

REFERENCES AND NOTES

1. S. Oome, G. Van den Ackerveken, *Mol. Plant Microbe Interact.* **27**, 1081–1094 (2014).
2. M. Gijzen, T. Nürnberger, *Phytochemistry* **67**, 1800–1807 (2006).
3. C. Ottmann *et al.*, *Proc. Natl. Acad. Sci. U.S.A.* **106**, 10359–10364 (2009).
4. D. Qutob *et al.*, *Plant Cell* **18**, 3721–3744 (2006).
5. G. Anderluh, J. H. Lakey, *Trends Biochem. Sci.* **33**, 482–490 (2008).
6. N. Rojko, M. Dalla Serra, P. Maček, G. Anderluh, *Biochim. Biophys. Acta* **1858**, 446–456 (2016).
7. B. Bakrač *et al.*, *J. Biol. Chem.* **283**, 18665–18677 (2008).
8. J. L. Cacas *et al.*, *Plant Physiol.* **170**, 367–384 (2016).
9. J. E. Markham, D. V. Lynch, J. A. Napier, T. M. Dunn, E. B. Cahoon, *Curr. Opin. Plant Biol.* **16**, 350–357 (2013).
10. L. Fang *et al.*, *Plant Cell* **28**, 2991–3004 (2016).
11. E. J. M. Van Damme *et al.*, *Eur. J. Biochem.* **202**, 23–30 (1991).
12. P. Ternes *et al.*, *New Phytol.* **192**, 841–854 (2011).
13. J. C. Mortimer *et al.*, *Plant Cell* **25**, 1881–1894 (2013).
14. S. König *et al.*, *New Phytol.* **196**, 1086–1097 (2012).
15. M. Nagano *et al.*, *Plant Cell* **28**, 1966–1983 (2016).
16. B. A. Bailey, *Phytopathology* **85**, 1250–1255 (1995).
17. J. L. Cacas *et al.*, *Phytochemistry* **96**, 191–200 (2013).
18. J. S. Griffitts *et al.*, *Science* **307**, 922–925 (2005).
19. D. G. Pina, L. Johannes, *Toxicon* **45**, 389–393 (2005).
20. C. Buré, J. L. Cacas, S. Mongrand, J. M. Schmitter, *Anal. Bioanal. Chem.* **406**, 995–1010 (2014).

ACKNOWLEDGMENTS

Work was supported by Deutsche Forschungsgemeinschaft (Nu70/1-9, SFB1101, INST 186/1167-1), Slovenian Research Agency (P1-0391, J1-7515), Seventh Framework Program BioStructX N°283570, Japan Ministry for Science and Technology JP16K08259, L'Agence Nationale de la Recherche (11-INBS-0010), U.S. Department of Energy Joint BioEnergy Institute (DE-AC02-05CH11231), Fonds de la Recherche Scientifique (Projet de Recherche grant T.1003.14, IAP P7/44 iPros), Belgian Program on Interuniversity Attraction Poles (IAPP7/44iPros), University of Liège (FIELD), RIKEN Integrated Lipidology Program, RIKEN Center for Sustainable Resource Science Wako, Platform Métabolome-Fluxome-Lipidome Bordeaux, and Göttingen Metabolomics and Lipidomics Platform. We thank Š. P. Novak, C. Thurow, N. Li, B. Thomma, G. Felix, M. Gijzen, A. Gust, J. Parker, T. Romeis, synchrotron Elletra, and the Graduate School of Biomedicine, University of Ljubljana (T.L.) for support. This work is dedicated to late Prof. Hanns Ulrich Seitz. All authors agreed on the manuscript. Structures are deposited (PDB: 5NNW, 5NO9). Supplementary materials contain additional data.

SUPPLEMENTARY MATERIALS

www.sciencemag.org/content/358/6369/1431/suppl/DC1
Materials and Methods
Figs. S1 to S15
Tables S1 and S2
References (*21*–*46*)

18 May 2017; accepted 31 October 2017
10.1126/science.aan6874

Eudicot plant-specific sphingolipids determine host selectivity of microbial NLP cytolysins

Tea Lenarcic, Isabell Albert, Hannah Böhm, Vesna Hodnik, Katja Pirc, Apolonija B. Zavec, Marjetka Podobnik, David Pahovnik, Ema Zagar, Rory Pruitt, Peter Greimel, Akiko Yamaji-Hasegawa, Toshihide Kobayashi, Agnieszka Zienkiewicz, Jasmin Gömann, Jenny C. Mortimer, Lin Fang, Adiilah Mamode-Cassim, Magali Deleu, Laurence Lins, Claudia Oecking, Ivo Feussner, Sébastien Mongrand, Gregor Anderluh and Thorsten Nürnberger

Science **358** (6369), 1431-1434.
DOI: 10.1126/science.aan6874

An extra sugar protects

Many microbial pathogens produce proteins that are toxic to the cells that they are targeting. Broad-leaved plants are susceptible to NLP (necrosis and ethylene-inducing peptide 1–like protein) toxins. Lenarcic *et al.* identified the receptors for NLP toxins to be GIPC (glycosylinositol phosphorylceramide) sphingolipids (see the Perspective by Van den Ackerveken). Their findings reveal why these toxins only attack broad-leaved plants (so-called eudicots): If the sphingolipid carries just two hexoses, as is the case for eudicots, the toxin binds and causes cell lysis. But in monocots with sphingolipids that have three hexoses, the toxin is ineffective.

Science, this issue p. 1431; see also p. 1383